SICE Annual Conference 2008
August 20-22, 2008, The University Electro-Communications, Japan

Dynamic Modeling and Sliding-Mode Control of a Ball Robot with Inverse Mouse-Ball Drive

Ching-Wen Liao, Ching-Chih Tsai*, Yi Yu Li, Cheng-Kai Chan

Department of Electrical Engineering, National Chung Hsing University
250, Kuo-Kuang Road, Taichung 40227, Taiwan, R.O.C.
*E-mail:cctsai@dragon.nchu.edu.tw

Abstract: This paper presents techniques for dynamic modeling and control of a Ball robot (Ballbot) with inverse mouse-ball drive that is accomplished by simultaneously activating two independent brushless motors. Under this driving scheme, a completely dynamic model of the robot moving in a flat terrain is established constructed based on Lagrangian mechanics. With the model, a sliding–mode control is proposed based on backstepping to accomplish robust balancing and agile path tracking of the robot with exogenous disturbances. Computer simulations are conducted for illustration of the effectiveness of the proposed modeling and control method.

Keywords: Ball robot, Lagrangian mechanics, modeling, path tracking, sliding-model.

1. INTRODUCTION

Ball robot (ballbot) with inverse mouse-ball drive, shown in fig. 1, has been constructed to accomplish effective interactions in human environments. To achieve efficient navigation around the human living space and establish friend and convenient man-machine interactions, this kind of robot must have high centers of gravity, narrow bases of support, agile mobility toward any poses, and dynamical stability. In [1], the authors used Lagrangian mechanics to derive a simplified dynamic equation of the robot driven by one dc motor at a time, and then employed this dynamic model employed to develop the LQR (linear quadratic regulator) control law in order to achieve stabilization and basic path tracking of the robot. However, the capabilities of such a controller fall short of robust balancing and agile mobility that will be required in order for a ballbot to operate effectively in human environments.

The objective of the paper is to present techniques for dynamic modeling, robust balancing and agile path tracking of a ballbot with inverse mouse-ball drive, which is accomplished by simultaneously activating two independent brushless motors. Under this driving scheme, the complete dynamic model of the robot moving in a flat terrain is constructed based on Newtonian mechanics. With the model, a sliding–mode control method is proposed based on backstepping to accomplish robust balancing and agile path tracking of the robot with unknown friction, parameters variations and exogenous disturbances. The merit and performance of the proposed control method are exemplified by conducting several computer simulations for the ballbot. The main contributions of the paper are twofold; one is the development of the dynamic model of the robot simultaneously driven by two independent brushless motors; the other is the design of the sliding-model controller to simultaneously achieve self-balancing and path tracking.

The rest of the paper is organized as follows. Section II is devoted to establishing the dynamic model of the robot with two independent brushless motors. In Section III, the sliding-mode controller is synthesized to achieve the design goals. Several computer simulations are performed in Section IV to illustrate the effectiveness of the proposed modeling and control method. Section V concludes the paper.

2. SYSTEM DESCRIPTION

The section will first describe the system structure and physical configuration of the designed ballbot, and then derive the dynamic model of the robot using Langrangian mechanics. Note that the modeling process is based on a simplification assumption that the ballbot is constructed by two major components: the cylinder and the ball, as Fig. 1 shows. Moreover, the cylinder is 1.5 m tall, with a diameter of 300 mm and a weight of 45 kg. The ball is a 220 mm diameter ball with a weight of 7.264 Kg (=16 lb). To describe the dynamics of the robot, a reference frame $\vec{a}_1$, $\vec{a}_2$, $\vec{a}_3$ together with a 3-1 Euler angle transformation(ϕ, θ) is used to orient the cylinder [2], as Fig. 2 shows. The angular velocity of the cylinder can be expressed as

$$w_c = \dot{\theta}\vec{a}_1'' + \dot{\phi}\sin(\theta)\vec{a}_2'' + \dot{\phi}\cos(\theta)\vec{a}_3'' \tag{1}$$

Let us write the kinetic and potential energies of the cylinder and the ball. For the ball we have

$$T_{ball} = \frac{1}{2}m_b(\dot{x}^2 + \dot{y}^2) + \frac{1}{2}I_b w_b^2, \quad V_{ball} = 0 \tag{2}$$

where I_b, m_b and r_b are, respectively the moment of inertia, mass, and radius of the ball. Assume no slip between the ball and the floor, the kinetic energies of the cylinder can be rewrite as

$$T_{ball} = \frac{1}{2}m_b(\dot{x}^2 + \dot{y}^2) + \frac{1}{2}I_b(\frac{\dot{x}^2}{r^2} + \frac{\dot{y}^2}{r^2}) \tag{3}$$

For the cylinder we have

$$T_{cylinder} = \frac{1}{2}[I_c\dot{\theta}^2 + I_c\dot{\phi}^2\sin^2(\theta) + I_{cz}\dot{\phi}^2\cos^2(\theta)] + \frac{1}{2}m_c(v_G \bullet v_G), \quad V_{cylinder} = m_c g l\cos(\theta) \tag{4}$$

where I_c, I_{cz} and m_c are the moments of inertia

and mass, the velocity of the center of mass of the cylinder is

$$v_G = \dot{x}\vec{a}_1 + \dot{y}\vec{a}_2 + \vec{w}_c \times \vec{l} = \dot{x}\vec{a}_1 + \dot{y}\vec{a}_2 + l\dot{\phi}\sin(\theta)\vec{a}_1'' - l\dot{\theta}\vec{a}_2'' \quad (5)$$

One expresses $\vec{a}_1''$ and $\vec{a}_2''$ by

$$\vec{a}_1'' = \cos(\phi)\vec{a}_1 + \sin(\phi)\vec{a}_2 \quad (6)$$

$$\vec{a}_2'' = -\sin(\phi)\cos(\theta)\vec{a}_1 + \cos(\phi)\cos(\theta)\vec{a}_2 + \sin(\theta)\vec{a}_3 \quad (7)$$

This results in the velocity expression for the center of mass of the cylinder, which is given by

$$v_G = [\dot{x} + l\dot{\phi}\sin(\theta)\cos(\phi) + l\dot{\theta}\sin(\phi)\cos(\theta)]\vec{a}_1 + [\dot{y} + l\dot{\phi}\sin(\theta)\sin(\phi) - l\dot{\theta}\cos(\phi)\cos(\theta)]\vec{a}_2 - l\dot{\theta}\sin(\theta)\vec{a}_3 \quad (8)$$

The total kinetic energy is

$$\begin{aligned} T &= T_{ball} + T_{cylinder} \\ &= (\frac{m_b}{2} + \frac{I_b}{2r^2})(\dot{x}^2 + \dot{y}^2) \\ &+ \frac{m_c}{2}[\dot{x} + l\dot{\phi}\sin(\theta)\cos(\phi) + l\dot{\theta}\sin(\phi)\cos(\theta)]^2 \\ &+ \frac{m_c}{2}[\dot{y} + l\dot{\phi}\sin(\theta)\sin(\phi) - l\dot{\theta}\cos(\phi)\cos(\theta)]^2 \\ &+ \frac{m_c}{2}[l\dot{\theta}\sin(\theta)]^2 + \frac{I_c}{2}\dot{\theta}^2 + \frac{I_c}{2}\dot{\phi}^2\sin^2(\theta) \\ &+ \frac{I_{cz}}{2}\dot{\phi}^2\cos^2(\theta) \end{aligned} \quad (9)$$

Define the Lagrangian L by $L = T - V_{cylinder}$ .The Euler-Lagrange equations of motion for the Ballbot model are

$$\begin{aligned} (I_c + M_c l^2)\ddot{\theta} &= T + (M_c l^2 + I_c)\dot{\phi}^2\sin(\theta)\cos(\theta) \\ &+ M_c lg\sin(\theta) - M_c l\ddot{x}\sin(\phi)\cos(\theta) \\ &+ M_c l\ddot{y}\cos(\phi)\cos(\theta) \end{aligned} \quad (10)$$

$$\begin{aligned} (I_c + M_c l^2)\ddot{\phi}\sin(\theta) &= -2(M_c l^2 + I_c)\dot{\phi}\dot{\theta}\cos(\theta) \\ &+ I_{cz}\dot{\phi}\dot{\theta}\cos(\theta) - M_c l\ddot{x}\cos(\phi)\sin(\theta) \\ &- M_c l\ddot{y}\sin(\phi)\sin(\theta) \end{aligned} \quad (11)$$

$$\begin{aligned} (M_c r - \frac{I_B}{r})\ddot{x} &= T\sin(\phi) - M_c rl[\ddot{\phi}\cos(\phi)\sin(\theta) \\ &+ 2\dot{\phi}\dot{\theta}\cos(\phi)\cos(\theta) + \ddot{\theta}\sin(\phi)\cos(\theta) \\ &- \dot{\phi}^2\sin(\phi)\sin(\theta) - \dot{\theta}^2\sin(\phi)\sin(\theta)] \end{aligned} \quad (12)$$

$$\begin{aligned} (M_c r - \frac{I_B}{r})\ddot{y} &= -T\cos(\phi) - M_c rl[\ddot{\phi}\sin(\phi)\sin(\theta) \\ &+ 2\dot{\phi}\dot{\theta}\sin(\phi)\cos(\theta) - \ddot{\theta}\cos(\phi)\cos(\theta) \\ &+ \dot{\phi}^2\cos(\phi)\sin(\theta) + \dot{\theta}^2\cos(\phi)\sin(\theta)] \end{aligned} \quad (13)$$

where T is the applied torque between the cylinder and body in the direction $\vec{a}_1''$. Substituting (12) and (13) into (10) gives

$$\begin{aligned} \ddot{\theta} &= \frac{(M_l r - \frac{I_B}{r}) - M_l l\cos(\theta)T}{[(M_l r - \frac{I_B}{r})I_1 - M_l^2 rl^2\cos^2(\theta)]} \\ &+ \frac{[(M_l r - \frac{I_B}{r})(I_1 - I_3) - M_l^2 rl^2]\sin(\theta)\cos(\theta)\dot{\phi}^2}{[(M_l r - \frac{I_B}{r})I_1 - M_l^2 rl^2\cos^2(\theta)]} \\ &- \frac{M_l^2 rl^2\sin(\theta)\cos(\theta)\dot{\theta}^2}{[(M_l r - \frac{I_B}{r})I_1 - M_l^2 rl^2\cos^2(\theta)]} \\ &+ \frac{(M_l r - \frac{I_B}{r})M_l lg\sin(\theta)}{[(M_l r - \frac{I_B}{r})I_1 - M_l^2 rl^2\cos^2(\theta)]} \end{aligned} \quad (14)$$

which is the balance dynamic equation of the cylinder. Let $\ddot{D}$ be $\frac{\ddot{x}}{\sin(\phi)} = \frac{-\ddot{y}}{\cos(\phi)}$, and $\dot{\phi}$ be equal to zero during the position control process, then (12) and (13) can be rewritten by

$$\begin{aligned} \ddot{D} &= \frac{T}{(M_c r - \frac{I_B}{r})} \\ &- \frac{M_c rl}{(M_c r - \frac{I_B}{r})}[\ddot{\theta}\cos(\theta) - \dot{\phi}^2\sin(\theta) - \dot{\theta}^2\sin(\theta)] \end{aligned} \quad (15)$$

which is the ballbot position equation.

3. CONTROLLER SYNTHESIS

The first part includes the paper title, authors' name, abstract, and keywords. All fonts must be in Times New Roman, and the font size of the title, authors' name, affiliation, abstract, and keywords are bold 12pt, 11pt, 10pt, 10pt, and 10pt respectively.

There are two goals of a controller for the ballbot; one is to maintain the robot without falling and the other is to drive the ballbot to achieve point-to-point control, or stabilization. Notice that the two goals must be done using only one degree of control, namely that this control problem falls into the category of the so-called underactuated control. Because the general sliding-mode control method is unable to achieve the design aims, a hierarchical sliding-mode control method studied in [3] will be employed; this controller consists of two layers, inner layer and outer layer. To design hierarchical sliding-mode controller, one defines two sliding functions in the inner layer by

$$S_{TH}(\theta) = \dot{\theta} + k_{TH}\theta \quad (16)$$

$$S_{PO}(D) = \dot{D} + k_{PO}(D - D_d) \quad (17)$$

Where D_d is the desired position, and k_{TH} and k_{PO} are two positive constants. Differentiating $S_{TH}(\theta)$ and $S_{PO}(D)$ obtains

$$\dot{S}_{TH}(\theta) = \ddot{\theta} + k_{TH}\dot{\theta} \quad (18)$$

$$\dot{S}_{PO}(D) = \ddot{D} + k_{PO}\dot{D} \quad (19)$$

Substituting (14) and (15) into (18) and (19), we have

$$\dot{S}_{TH}(\theta)=\frac{(M_l r-\frac{I_B}{r})-M_l l\cos(\theta)T}{[(M_l r-\frac{I_B}{r})I_1-M_l^2 rl^2\cos^2(\theta)]}+\frac{[(M_l r-\frac{I_B}{r})(I_1-I_3)-M_l^2 rl^2]\sin(\theta)\cos(\theta)\dot{\phi}^2}{[(M_l r-\frac{I_B}{r})I_1-M_l^2 rl^2\cos^2(\theta)]}-\frac{M_l^2 rl^2\sin(\theta)\cos(\theta)\dot{\theta}^2}{[(M_l r-\frac{I_B}{r})I_1-M_l^2 rl^2\cos^2(\theta)]}+\frac{(M_l r-\frac{I_B}{r})M_l lg\sin(\theta)}{[(M_l r-\frac{I_B}{r})I_1-M_l^2 rl^2\cos^2(\theta)]}+k_{TH}\dot{\theta} \tag{20}$$

$$\dot{S}_{PO}(D)=\frac{T}{(M_c r-\frac{I_B}{r})}+k_{PO}\dot{D} \tag{21}$$

$$-\frac{M_c rl}{(M_c r-\frac{I_B}{r})}[\ddot{\theta}\cos(\theta)-\dot{\phi}^2\sin(\theta)-\dot{\theta}^2\sin(\theta)]$$

From (20) and (21), it is easy to find out the subsequent equivalent control of the inner layer by setting (20) and (21) to be zero.

$$T_{TH}=[-k_{TH}\dot{\theta}]\frac{[(M_c r-\frac{I_B}{r})(I_c+M_c l^2)-M_c^2 rl^2\cos^2(\theta)]}{(M_c r-\frac{I_B}{r})-M_c l\cos(\theta)}+\frac{M_c^2 rl^2\sin(\theta)\cos(\theta)}{(M_c r-\frac{I_B}{r})-M_c l\cos(\theta)}\dot{\theta}^2-\frac{(M_c r-\frac{I_B}{r})M_l lg}{(M_c r-\frac{I_B}{r})-M_c l\cos(\theta)}\sin(\theta)-\frac{[(M_c r-\frac{I_B}{r})(I_c+M_c l^2-I_{cz})-M_c^2 rl^2]\sin(\theta)\cos(\theta)}{(M_c r-\frac{I_B}{r})-M_c l\cos(\theta)}\dot{\phi}^2 \tag{22}$$

$$T_{PO}=M_c rl[\ddot{\theta}\cos(\theta)-\dot{\phi}^2\sin(\theta)-\dot{\theta}^2\sin(\theta)]-(M_c r-\frac{I_B}{r})k_{PO}\dot{D} \tag{23}$$

Next, define the sliding function of the outer layer by

$$S=\alpha S_{TH}(\theta)+\beta S_{PO}(D) \tag{24}$$

where α and β are two positive real numbers. Defined the total torque T

$$T=T_{TH}+T_{PO}+T_S \tag{25}$$

Where T_S is the switch torque. In order to make the second layers sliding function converged to zero, the following Lyapunov function is chosen by

$$V(t)=\frac{S^2}{2} \tag{26}$$

which leads to the time derivative of $V(t)$ with respect to time yields

$$\dot{V}(t)=S\dot{S} \tag{27}$$

Let $\dot{S}$ be

$$\dot{S}=-\eta\times\mathrm{sgn}(S)-k\times S \tag{28}$$

where $\mathrm{sgn}(\bullet)$ is the signum function, and η and k are two positive numbers. If $\dot{S}$ satisfies equation (28), then equation (27) becomes

$$\begin{aligned}\dot{V}(t)&=S(-\eta\times\mathrm{sgn}(S)-k\times S)\\&=-\eta|S|-kS^2<0,\quad if\quad S\neq 0\end{aligned} \tag{29}$$

Barbalat's lemma implies that $V(t)$ and S will converge to zero as time approached infinity. The substitution of (20) ~ (25) into equation (28) results in

$$T_S=-\frac{T_{S1}}{T_{S2}} \tag{30}$$

where

$$T_{S1}=\alpha[(M_c r-\frac{I_B}{r})I_1-M_c^2 rl^2\cos^2(\theta)]T_{PO}+[\beta(M_c r-\frac{I_B}{r})T_{TH}+\eta\times\mathrm{sgn}(S)+k\times S][(M_c r-\frac{I_B}{r})-M_c l\cos(\theta)] \tag{31}$$

$$T_{S2}=\alpha[(M_c r-\frac{I_B}{r})I_1-M_c^2 rl^2\cos^2(\theta)]+\beta(M_c r-\frac{I_B}{r})[(M_c r-\frac{I_B}{r})-M_c l\cos(\theta)] \tag{32}$$

By substituting (22), (23) and (30) into (25), we have the total torque T

$$T=\frac{T_1}{T_2} \tag{33}$$

where

$$\begin{aligned}T_1=&\alpha[(M_c r-\frac{I_B}{r})I_1-M_c^2 rl^2\cos^2(\theta)]T_{TH}\\&+\beta(M_c r-\frac{I_B}{r})[(M_c r-\frac{I_B}{r})-M_c l\cos(\theta)]T_{PO}\\&-[(M_c r-\frac{I_B}{r})-M_c l\cos(\theta)][\eta\times\mathrm{sgn}(S)+k\times S]\end{aligned} \tag{34}$$

$$\begin{aligned}T_2=&\alpha[(M_c r-\frac{I_B}{r})I_1-M_c^2 rl^2\cos^2(\theta)]\\&+\beta(M_c r-\frac{I_B}{r})[(M_c r-\frac{I_B}{r})-M_c l\cos(\theta)]\end{aligned} \tag{35}$$

4. SIMULATION RESULTS

This section will examine the performance of the proposed controller, compare such a controller with a controller designed based on the decoupled model. In computer simulation, the friction between the cylinder and the ball is ignored. The initial conditions are $\theta=10(\mathrm{deg})$, $\dot{\theta}=0$, $\phi=135(\mathrm{deg})$ and $\dot{\phi}=500(\mathrm{deg/sec})$. The parameters of the proposed controller are set by $K_{TH}=10$, $K=10$ and $\eta=10$. The simulation results of both controllers for balancing are depicted in Figs. 3 and 4. The results indicate that the proposed controller outperforms that designed by the decoupled model in term of transient responses.

Next, explore the effectiveness of the proposed controller by steering the robot from a starting point to a destination, i.e., point-to-point stabilization or regulation. In doing so, the initial conditions are $\theta=0$, $\dot{\theta}=0$, $\phi=0$ and $\dot{\phi}=0$, and the parameters of the controller are $\alpha=1.8$, $\beta=1.5$

$K_{TH}=5$, $K_{PO}=0.8$, $K=1$, $\eta=1$; the initial and final values of D are respectively given by $D=0$ $D=1$(unit: meter). Figs. 5, 6 and 7 displays the time behavior of the sliding functions, $\dot{\theta}$, θ , the position and velocity of the ballbot during point-to-point stabilization. Through the computer simulations, the proposed controller is shown to be capable of steering this kind of robot to the desired position in five seconds.

5. CONCLUSIONS

This paper has presented techniques for dynamic modeling and control of a Ballbot with inverse mouse-ball drive accomplished by simultaneously activating two independent brushless motors. The completely dynamic model of the robot moving in a flat terrain has been derived based on Lagrangian mechanics, and the hierarchical sliding–mode controller has been proposed to accomplish robust balancing and point-to-point stabilization of the robot in presence of exogenous disturbances. The effectiveness of the proposed modeling and control method has been exemplified by conducting computer simulations on the ballbot for accomplishing self-balancing and point-to-point movement. Interesting topics for future research would be to implement the proposed control scheme and then to develop an adaptive sliding mode control method and an autonomous navigation scheme for the robot.

ACKNOWLEDGEMENTS

The authors deeply acknowledge the final support in part from national science council, Taiwan, ROC, under contract 96-2221-E-005-106-MY2, and in part from the ministry of education, Taiwan, ROC, under ATU plan.

REFERENCES

[1] T. B. Lauwers, G. A. Kantor, R. L. Hollis, “A dynamical stable single-wheeled mobile robot with inverse mouse-ball drive,” *Proceedings of the IEEE International Conference on Robotics and Automation,* pp. 2884-2889, May 2006.

[2] Haim Baruh “Analytical Dynamics”, McGraw-Hill Inc, 1999.

[3] W.wang, J.Yi, D.zhao, and D.Liu, “Design of a stable sliding-mode controller for a class of second-order underactuated systems ,” *IEE Proceeding of Control Theory and Applications,* vol.151, pp. 683-690, Nov.2004.

[4] Shaw jiun shiang and Huang bo kai,“Balance and trajectory tracking control for ball robot ”, *The 27th Chinese Institute of Engineers Conference*, B17-0046, Nov.2007

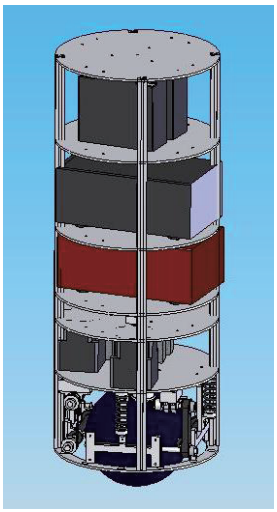

Fig. 1 Conceptual diagram of a ballbot.

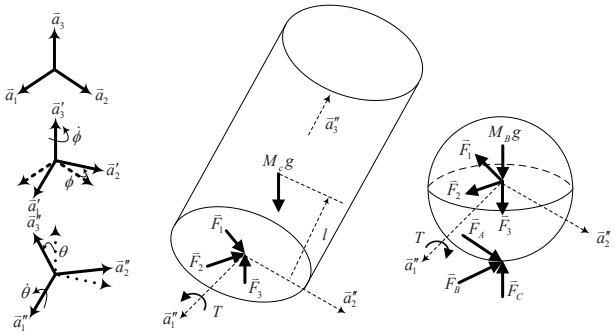

Fig. 2 Free-body diagrams.

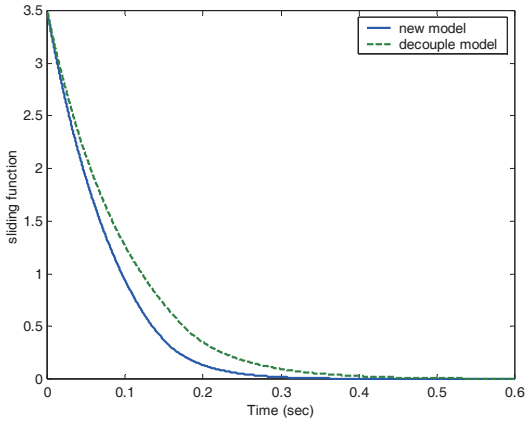

Fig. 3 Caption should be placed after the figure. Time behavior of the sliding function of the ballbot for self-balancing.

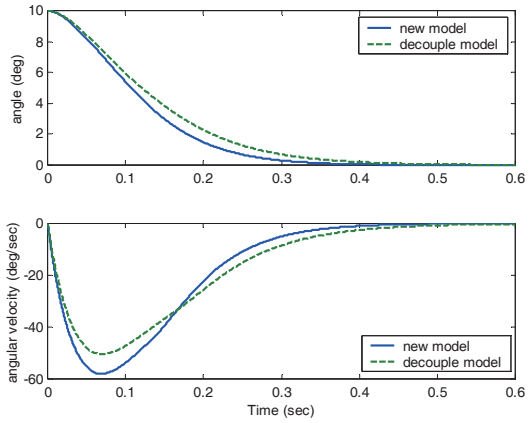

Fig. 4 Balancing simulation results for $\dot{\theta}$ and θ of the ballbot for self-balancing.

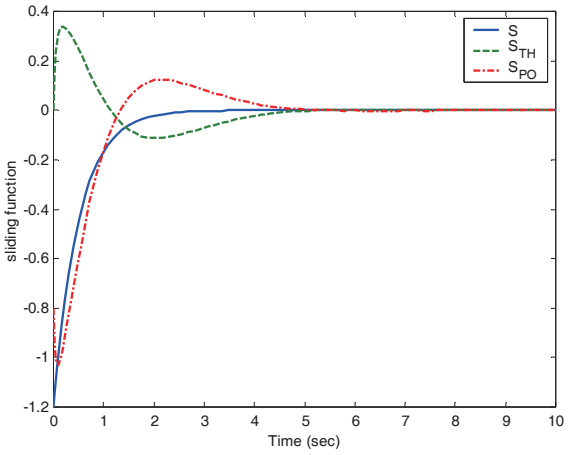

Fig. 5 Time behavior of the sliding functions of the ballbot during point-to-point stabilization .

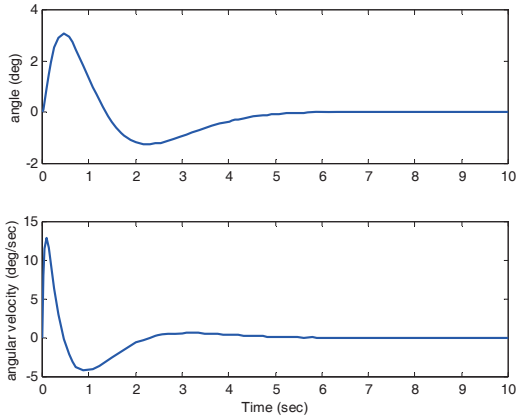

Fig. 6 Balancing simulation results for $\dot{\theta}$ and θ of the ballbot during point-to-point stabilization.

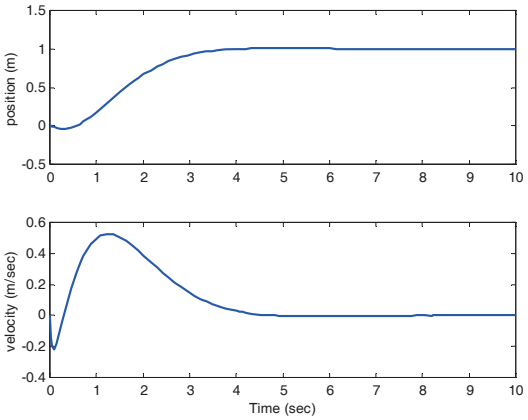

Fig. 7 Simulated position and velocity of the ballbot during point-to-point stabilization.